Wide Bandwidth Traveling-Wave InGaAsP/InP Electroabsorption Modulator for Millimeter Wave Applications

G. L. Li, S. A. Pappert*, C. K. Sun*, W. S. C. Chang, and P. K. L. Yu

University of California, San Diego; Department of ECE; La Jolla, CA 92093-0407
*SPAWAR Systems Center; San Diego, CA 92152-5001

***Abstract* — Traveling wave electroabsorption modulators (TW-EAMs) can provide large modulation bandwidth and high efficiency features for both analog and digital fiber-optic links. Here, high efficiency TW-EAMs with modulation bandwidths in excess of 40 GHz have been demonstrated. Observing the predicted bandwidth reduction for counter-propagating optical and microwave fields along the waveguide has validated the traveling-wave nature of the modulator.**

I. INTRODUCTION

High speed and high efficiency electroabsorption modulators (EAMs) are desirable for both analog and digital fiber-optic links. We have previously reported [1] that for maximum RF modulation efficiency, the EAM waveguide is typically limited to 200 ~ 300 μm in length due to the optical propagation loss in the waveguide. This maximum modulator length limitation also applies to digital link applications where the optical insertion loss of the EAM must be kept low. Our waveguide width is typically designed at ~3 μm in order to achieve good optical coupling efficiency with lensed fibers. However, for a lumped-element EAM with 200 μm long and 3 μm wide waveguide, the modulation bandwidth hardly exceeds 20 GHz even when a 50-Ω shunt resistance is used. To achieve a broader bandwidth, one can either shorten the waveguide length, reduce the waveguide width, increase the waveguide intrinsic layer thickness, or use a smaller shunt resistance. All of these approaches result in a significant penalty in modulation efficiency. In the past, much attention has been paid to short EAM waveguides for providing larger bandwidth [2-4]. The short-waveguide approach compromises modulation efficiency due to both shorter modulation length and smaller power handling ability. In digital links, an EAM with very short waveguide may not be able to provide large enough extinction ratio. The bandwidth for a lumped-element EAM is limited by the RC-time constant. To overcome the RC bandwidth limit without severely compromising the modulation efficiency, the traveling wave electroabsorption modulator (TW-EAM) has been proposed and experimentally investigated by several authors [5-7]. A major challenge of TW-EAM has been the design of a TW structure that will yield high modulation efficiency via large overlap of the modulation field with a thin intrinsic EA layer and a sufficiently high impedance for broadband match to the source with low attenuation at high frequencies. However, to our knowledge, the highest 3-dB electrical bandwidth published for TW-EAM is below 30 GHz [6,7]. This indicates that the potential of the traveling-wave effect has not been fully exploited. In [1], we have proposed several approaches for realizing a high efficiency TW-EAM with bandwidth above 50 GHz. Several important design issues have also been discussed in a later work [8].

In this work, following [1] and [8], we design and fabricate a broadband TW-EAM using the low-impedance termination approach. Excellent DC characteristics are measured for the TW-EAM devices fabricated, indicating high modulation efficiency is achievable. The measured modulation bandwidth for some of the devices is above 40 GHz, limited by the bandwidth of the measurement equipment. Bandwidth reduction is observed when the optical wave and microwave counter-propagate along the waveguide, which is consistent with the traveling-wave effect.

II. DEVICE DESIGN

The optical waveguide geometry for the TW-EAM is designed for maximum modulation efficiency. Fig. 1 shows the waveguide cross-section. The fabrication of the modulator ridge waveguides is done using wet chemical etching. The top metal width (w) is set at 3 μm, and is the same as the waveguide width due to the very smooth sidewall and vertical etching profile of the waveguide mesa.

The intrinsic bulk-InGaAsP (bandgap ~ 1.24 μm) absorption layer thickness is 0.35 μm thick. The absorption layer is sandwiched between two ~1 μm thick doped InGaAsP large optical cavity layers for good coupling efficiency with lensed fibers. TW-EAMs with waveguide

0-7803-6540-2/01/$10.00 (C) 2001 IEEE

lengths of 150 μm, 200 μm and 300 μm, are tested. Fig. 2 shows the top view of the TW-EAM device. 50-Ω CPW microwave connection transmission lines on semi-insulating InP substrate are implemented at the source and the terminator ports to make the electrical connection between the waveguide and microwave probes. Metal connections are made via the polyimide bridges.

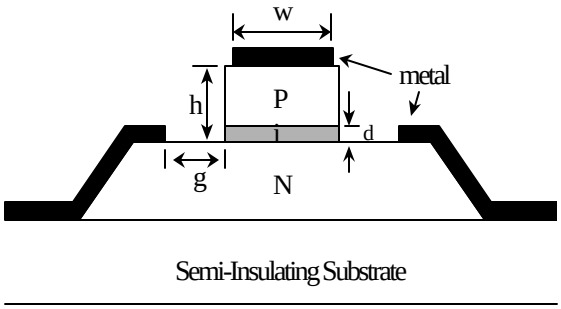

Fig. 1. Cross-section of the TW-EAM waveguide

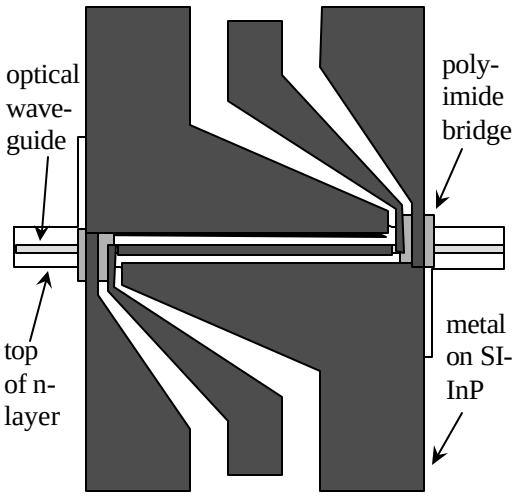

Fig. 2. Top view of the TW-EAM device design.

III. Measurement Results

A. DC Characteristics

The TW-EAM devices fabricated show good DC characteristics. For a device with 200 μm long modulator length plus 100 μm long passive waveguide (caused by inaccurate cleaving), the fiber-to-fiber optical insertion loss at zero bias is measured to be 11.3 dB with 1.32 μm wavelength light. Smaller insertion loss can be achieved with more accurate cleaving and anti-reflection coating at the facets. The maximum slope efficiency for the transfer curve normalized at zero bias is measured at 0.65 V^{-1} when the device is biased at −0.8 V. The normalized modulator DC transfer curve remains the same with the optical input power increased up to 20 mW. Since the modulation efficiency is determined by the modulator optical insertion loss, the slope of the transfer curve and the optical saturation power, the above reported DC characteristics result in excellent modulation efficiency for the TW-EAM device.

B. Modulation Frequency Response

A 40 GHz network analyzer HP8510B is used to measure the device frequency response. During the measurement, the terminator port of the TW-EAM devices is contacted by a resistor-shunted 50 GHz CPW microwave probe. The 2.4 mm connector of this probe is terminated by a 50 Ω resistor, giving a total termination impedance of 26.2 Ω for the TW-EAM devices. It is found that the frequency response curves show a low frequency roll-off due to the passive waveguide. This can be explained in light of the absence of metal on top of the passive waveguide, and the p-type layers are relative resistive at frequencies above 5 GHz. For example, for a device with a 150 μm long modulator section and 90 μm long passive waveguide, the effective modulation length is ~240 μm for frequencies below ~0.2 GHz and 150 μm for frequencies above 5 GHz. This modulation length changes give rise to the apparent low frequency roll off (20*log (240/150) = 4.1 dB) The low frequency roll-off characteristic can be eliminated by more accurate cleaving.

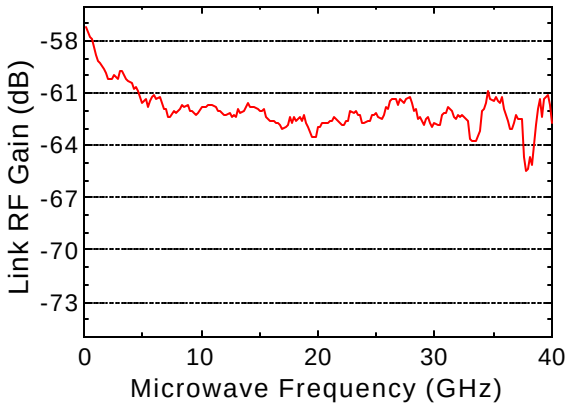

Fig. 3. Frequency response for a 150 μm long TW-EAM with 90 μm long passive waveguide. The input optical power is 11 dBm, detector responsivity is ~0.12 A/W up to 40 GHz.

The measured frequency response for a 150 μm long TW-EAM device (with 90 μm long passive waveguide) combined with the photodetector loss is shown in Fig. 3. For this measurement, the microwave probe at the source port has been calibrated out. Above 5 GHz, the frequency response does not roll off up to 40 GHz, indicating a modulation bandwidth of above 40 GHz for this TW-EAM device. The frequency response dip at 38 GHz is caused by the detector frequency response. For the 200 μm long device mentioned above, the 3-dB bandwidth is measured at ~35 GHz (as shown in top curve of Fig. 4).

It should be noted that the link RF gain in Fig. 3 can be improved 16.5 dB if a photodetector with responsivity of 0.8 A/W is used, instead of one with 0.12 A/W responsivity. Anti-reflection coating on the device facets can improve the link RF gain by another ~6 dB, and accurate cleaving can reduce ~2 dB RF loss (due to the ~1 dB optical loss in the passive waveguide). With these improvements, the link RF gain will be around –37 dB at 40 GHz for the 150 μm long device, with 11 dBm optical power input.

Previously, our group has reported a link RF gain of -17.4 dB for a lumped-element EAM at 1 GHz frequency (AR-coated, with detector responsivity ~0.8 A/W and input optical power 43 mW or 16.3 dBm) [9]. The corresponding link RF gain for this lumped-element EAM would be –34 dB if the optical power is scaled down to 11 dBm and a 50-Ω shunt resistor is used (which adds 6 dB RF loss at low frequency).

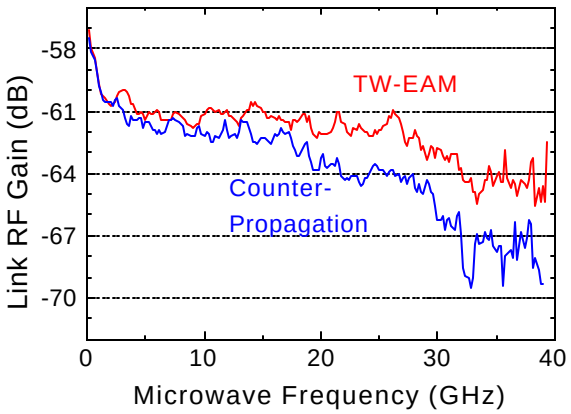

Fig. 4. Frequency response for a 200 μm long TW-EAM with 100 μm long passive waveguide.

C. Counter-Propagation Measurement

In order to confirm the traveling-wave effect in the device, we reverse the optical wave propagation direction for the 200 μm long device so that the optical wave and microwave counter-propagate along the waveguide. In this case the 3-dB bandwidth is measured at ~25 GHz, which is 10 GHz smaller than the ~35 GHz bandwidth of the normal TW-EAM device. The measured frequency responses are shown in Fig. 4. The bandwidth reduction in the counter-propagation measurement is consistent with the traveling-wave effect predicted for TW-EAM.

D. Return Loss

The return loss (S_{11}) of an EAM is often an important concern in a practical system. The desirable S_{11} is as small as possible, so that the microwave source will not be affected by the reflected microwave power. By using a 50-Ω shunt resistor for lumped-element EAMs, very small S_{11} can be achieved at low frequency. However, at high frequency, the impedance of the EAM is very small (~5 Ω for a 200 μm long and 3 μm wide waveguide), so that the 50-Ω shunt resistor does not help much to reduce S_{11}. This is illustrated in Fig. 5. The measured S_{11} for the TW-EAM device terminated with 26.2 Ω is also shown in the same figure. An interesting observation is that a smaller S_{11} is obtained for the TW-EAM device at frequencies above 5 GHz. This can be explained by the fact that the input impedance of the terminated TW-EAM device has different frequency dependence than that of the lumped-element EAM [1].

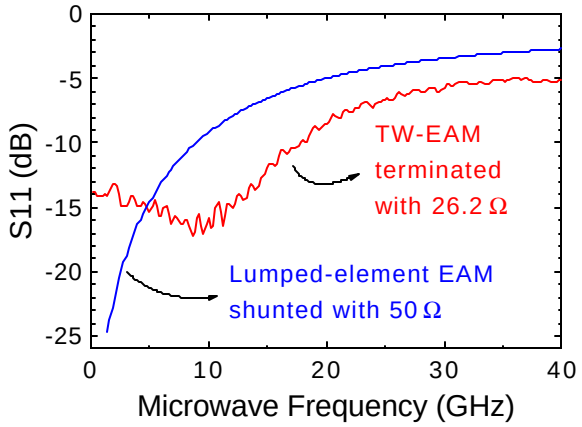

Fig. 5. Measured S_{11} of the TW-EAM compared with calculated S_{11} for lumped-element EAM shunted with 50-Ω.

E. Microwave Properties of the Waveguide

In terms of microwave properties, the TW-EAM waveguide shown in Fig. 1 is different from either a co-planar waveguide or a micro-strip waveguide. The microwave velocity is much slower in the TW-EAM

waveguide due to larger capacitance [1,5]. The TW-EAM modulation frequency response is determined by the waveguide microwave properties, including waveguide impedance, microwave velocity and microwave loss [1]. To measure these microwave parameters, the TW-EAM device can be treated as a two-port microwave device due to the electrode design shown in Fig. 2. The two-port S-parameters can be measured for TW-EAM devices with different waveguide length, so that the effect of the contact pads can be calibrated out and the microwave properties for the waveguide can be extracted. The extracted microwave parameters for the waveguide can be fed into the theoretical formula in [1] to calculate the modulation frequency response. In this way, the theory can be compared with the measurement results. Fig. 6 shows the typical microwave loss (or S_{21}) measured for TW-EAM devices with different waveguide length. From this figure we can see that the microwave loss due to the waveguide is pretty small. The parameter-extraction for the microwave properties of the waveguide will be presented at the conference.

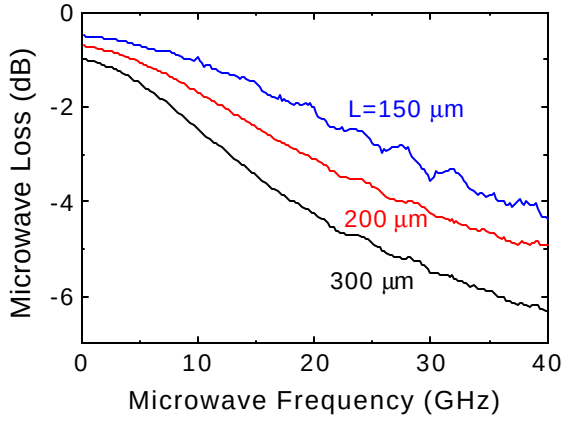

Fig. 6 Measured microwave loss for TW-EAM devices with different waveguide length.

IV. CONCLUSION

Wide bandwidth and high efficiency TW-EAM devices have been designed and fabricated according to our previously proposed low-impedance-termination approach. For the 150 µm long device, an electrical modulation bandwidth is measured above 40 GHz, limited by the measurement equipment. As expected, bandwidth reduction is observed when the optical wave and microwave counter-propagate along the waveguide. The modulation efficiency at 40 GHz for our TW-EAM is comparable to the modulation efficiency at low frequency for the reported lumped-element EAM using the same measurement setting. Improvement in modulation efficiency can be obtained by employing multiple quantum wells in the modulation layer. The results indicate that the traveling-wave EAM design is a very promising and practical approach for broadband millimeter wave as well as high-speed communication applications.

ACKNOWLEDGEMENT: This work is supported by AFRL, ONR and MICRO/Raytheon Program of California. The authors also wish to thank the following colleagues at UCSD and SPAWAR for their assistance: D. S. Shin, F. Lu, Y. M. Kang, P. Mages, R. Nguyen and Y. Wu.

REFERENCES

[1] G. L. Li, C. K. Sun, S. A. Pappert, W. X. Chen and P. K. L. Yu, "Ultra high-speed traveling wave electroabsorption modulator: design and analysis," *IEEE Trans. MTT, Special issue on "Microwave and Millimeter Wave Photonics"*, vol. 47, pp. 1177-1183, 1999.

[2] K. K. Loi, X. B. Mei, J. H. Hodiak, C. W. Tu and W. S. C. Chang, **"**38 GHz bandwidth 1.3 µm MQW electroabsorption modulators for RF photonic links," *Electron. Lett.*, vol. 34, pp. 1018-1019, 1998.

[3] T. Ido, S. Tanaka, M. Suzuki, M. Koizumi, H. Sano and H. Inoue, "Ultra-high-speed multiple-quantum-well electro-absorption modulators with integrated waveguides," *IEEE J. Lightwave Technol.*, vol. 14, pp. 2026-2034, 1996.

[4] A. Stöhr, R. Heinzelmann, R. Buß and D. Jäger, "Electroabsorption Modulators for Broadband Fiber Electro-Optic Field Sensors," *Applications of Photonic Technology 2, Plenum Press*, pp. 871-876, 1997.

[5] H. H. Liao, X. B. Mei, K. K. Loi, C. W. Tu, P. M. Asbeck and W. S. C. Chang, **"**Microwave structures for traveling-wave MQW electro-absorption modulators for wide band 1.3 µm photonic links," *Proc. SPIE, Optoelectronic Integrated Circuits*, vol. 3006, pp. 291-300, 1997.

[6] K. Kawano, M. Kohtoku, M. Ueki, T. Ito, S. Kondoh, Y. Noguchi and Y. Hasumi, **"**Polarisation-insensitive traveling-wave electrode electroabsorption (TW-EA) modulator with bandwidth over 50 GHz and driving voltage less than 2 V," *Electron. Lett.*, vol. 33, pp. 1580-1581, 1997

[7] S. Z. Zhang, Y. J. Chiu, P. Abraham and J. E. Bowers, "25-GHz Polarization-insensitive electroabsorption modulators with traveling-wave electrodes," *IEEE Photon. Technol. Lett.*, vol. 11, pp.191-193, 1999.

[8] G. L. Li, D. S. Shin, W. S. Chang, P. M. Asbeck, P. K. L. Yu, C. K. Sun, S. A. Pappert and R. Nguyen, "Design and fabrication of traveling wave electroabsorption modulator," *Proc SPIE*, vol. 3950, pp. 252-255, 2000.

[9] R. B. Welstand, S. A. Pappert, C. K. Sun, J. T. Zhu, Y. Z. Liu and P. K. L. Yu, "Dual-function electroabsorption waveguide modulator/detector for optoelectronic transceiver applications," *IEEE Photon. Technol. Lett,*, vol.8, pp.1540-1542,1996.